DOI: 10.1002/ejic.200900789

Bis(oxazolinylmethyl) Derivatives of C_4H_4E Heterocycles (E = NH, O, S) as C_2-Chiral Meridionally Coordinating Ligands for Nickel and Chromium

Felix Konrad,[a] Julio Lloret Fillol,[a] Christoph Rettenmeier,[a] Hubert Wadepohl,[a] and Lutz H. Gade*[a]

Keywords: N ligands / Chirality / Nickel / Chromium / Structure elucidation

The synthesis of the three ligands employed in this study is based on the condensation of two molar equivalents of (*S*)-valinol with the diester precursors pyrrole-2,5-bis(ethyl)acetate (**2a**), furan-2,5-bis(ethyl)acetate (**2b**) and thiophene-2,5-bis(ethyl)acetate (**2c**). This gave the corresponding bis(oxazolinylmethyl)pyrrole (*i*PrL$_N$H, **4a**), bis(oxazolinylmethyl)-furan (*i*PrL$_O$, **4b**) and bis(oxazolinylmethyl)thiophene (*i*PrL$_S$, **4c**) ligands. Stirring **4a** in MeOD at ambient temperature in the presence of a catalytic amount of acetic acid (1 mol-%) led to complete hydrogen/deuterium exchange in the two bridging methylene groups of the ligand. This behaviour is explained by an acetate-mediated reversible proton transfer between the oxazoline N atom and the methylene bridge, a conjecture which was supported by a DFT study of the process. Deprotonation of *i*PrL$_N$H (**4a**) with *t*BuLi at –78 °C and subsequent stirring with $NiCl_2$ yielded the square planar nickel(II) complex [Ni(*i*PrL$_N$)Cl] (**5**). However, on stirring *i*PrL$_N$H (**4a**) with nickel acetate in methanol, a deep red nickel acetato complex [Ni(*iso*-*i*PrL$_N$)(OAc)] (**6**) bearing the isomerized tridentate pincer ligand was obtained. Reaction of acetato complex **6** with Me_3SiCl in dichloromethane cleanly gave the corresponding chlorido complex [Ni(*iso*-*i*PrL$_N$)Cl] (**7**), which is the isomer of compound **5**. The intra-ligand rearrangement was explained by acetate-mediated proton transfer between the methylene bridges and the 3/4-positions of the pyrrole ring, the computed thermodynamic driving force being ΔG = –9.8 kcal mol^{-1}. Neither thiophene derivative **4c** nor furan-derived ligand **4b** gave robust, isolable complexes with nickel(II). However, reaction of *i*PrL$_O$ (**4b**) with [$CrCl_3$(thf)$_3$] in thf yielded the yellow-green complex [$CrCl_3$(*i*PrL$_O$)] (**8**), whereas no complexation occurred with the analogous thiophene-derived bisoxazoline **4c**.

Introduction

Next to Nishiyama's bis(2-oxazolinyl)phenyl (phebox) ligands,[1] there are only a few chiral monoanionic meridionally coordinating ligands, frequently referred to as "pincers",[2] which have given rise to highly enantioselective transition-metal catalysts. Instead of cyclometallations, which are feasible only with certain transition metals, the use of central heterocyclic units that can be deprotonated or that contain a potentially ligating central atom, as in the case of the ubiquitous pybox ligand,[3] allows greater flexibility in constructing new molecular catalysts. This construction principle is illustrated by the three structurally closely related ligands **Ia**–**c** which are bisoxazolines containing a rigid central dibenzopyrrole (**Ia**, acting as protioligand), dibenzofuran (**Ib**) and dibenzothiophene (**Ic**) backbone.

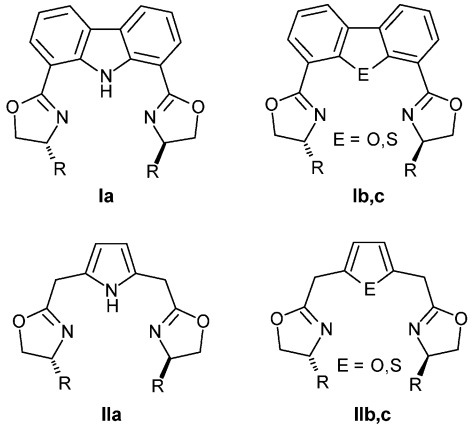

Dibenzopyrrole-derived ligand **Ia** was reported by Nakada et al. in 2003[4] and was employed in chromium(III)-catalyzed Nozaki–Hiyama allylations, affording high yields and enantioselectivities. Earlier, Kanemasa et al. had reported compound **Ib** ("dbfox"), which they coordinated to various transition metals and used in enantioselective Diels–Alder reactions of cyclopentadiene with 3-acryloyl-2-oxazolidinone; the nickel(II) complex [(**Ib**)Ni(H_2O)$_3$]-

[a] Anorganisch-Chemisches Institut, Universität Heidelberg, Im Neuenheimer Feld 270, 69120 Heidelberg, Germany
E-mail: lutz.gade@uni-hd.de
Supporting information for this article is available on the WWW under http://dx.doi.org/10.1002/ejic.200900789.

$(ClO_4)_2$ gave the best results.[5] Finally, ligand **Ic** ("dbt-box"), reported by Schulz et al. induced high enantioselectivities and gave high yields in the palladium-catalyzed allylic substitution of 1,3-diphenyl-2-propenylacetate with dimethyl malonate.[6]

We recently reported the synthesis of 2,5-bis(2-oxazolinylmethyl)pyrroles **IIa** and their coordination to palladium(II)[7] and rhodium(I/III).[8] They are readily obtained by condensation of pyrrole-2,5-diethyl acetate with two molar equivalents of a chiral amino alcohol. A particularly characteristic pattern of reactivity observed in complexes containing **IIa** is the tendency of intraligand rearrangements, leading to planar, conjugated π-systems despite the fact that the associated 1,3-H shifts are orbital symmetry forbidden processes for the noncoordinated ligand. In this work, we provide evidence for a nonconcerted protolytic mechanism for this rearrangement in the presence of catalytic amounts of a carboxylic acid such as acetic acid. Furthermore, we extend the ligand design principle to 2,5-bis(2-oxazolinylmethyl)furans **IIb** and 2,5-bis(2-oxazolinylmethyl)thiophenes **IIc**, which can act as neutral tridentate ligands. Furthermore, a study into the coordination chemistry of **IIa** with nickel has provided insight into the reactivity of the ligand system upon its coordination to a transition metal, whereas first results concerning the coordination of **IIb** and **IIc** indicate the limitations of the chosen approach.

Results and Discussion

Synthesis of the Bis(oxazolinylmethyl)pyrrole ("pyrrmebox"), Bis(oxazolinylmethyl)furan ("furmebox") and Bis(oxazolinylmethyl)thiophene ("thiomebox") Ligands

The synthesis of the three ligands employed in this study is similar and based on the condensation of two molar equivalents of (*S*)-valinol with diester precursors **2a**–**c**, all three of which were obtained by cyclization of the same 1,4-diketone derivative **1** (Scheme 1).

The synthesis of pyrrole derivative **2a** by Paal–Knorr-type cyclization was reported previously by us[8] and is based on an earlier protocol by Brooker et al.[9a] Compounds **2b** and **2c** are reported in the literature,[9d,9e] albeit by different synthetic routes and by using different precursor materials, which gave both in lower yield. In the case at

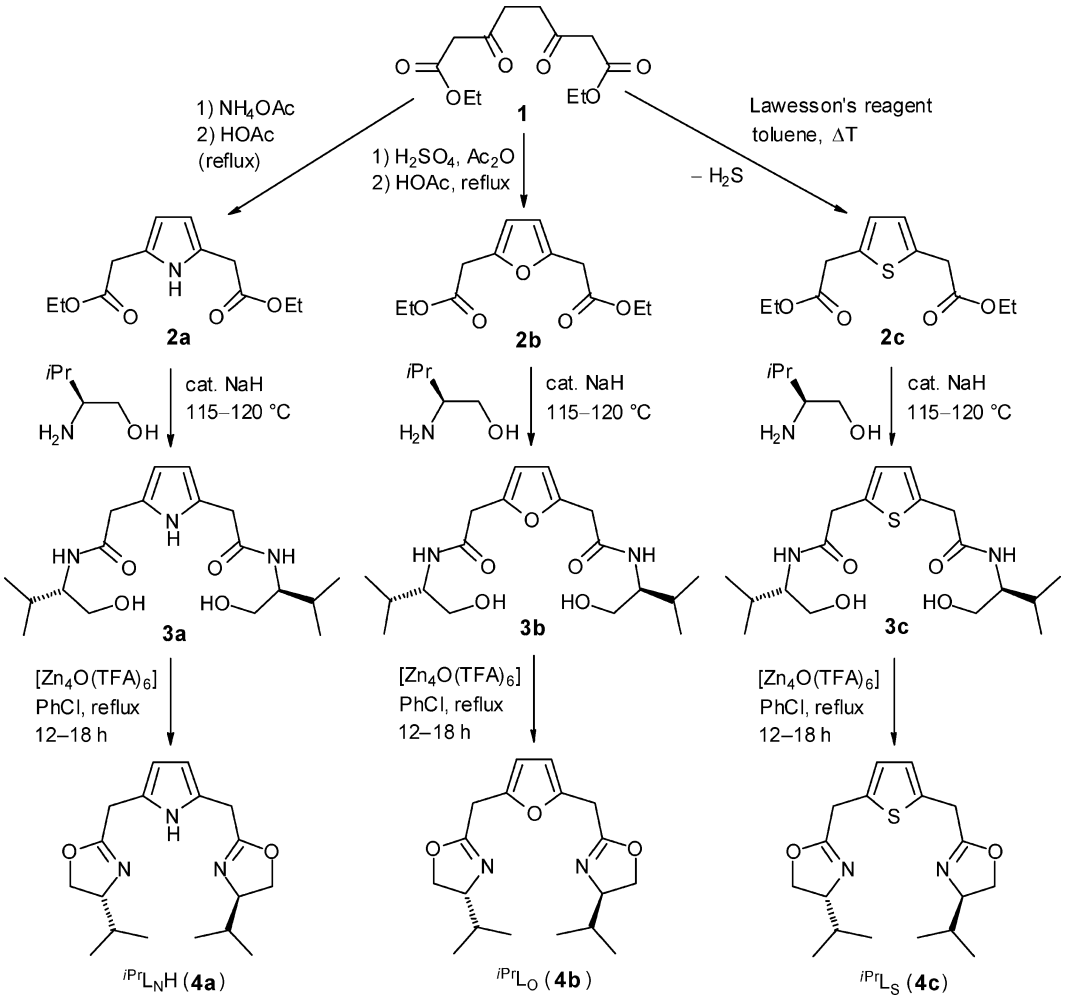

Scheme 1. Synthesis of the bis(oxazolinylmethyl) derivatives of C_4H_4E heterocycles (E = NH: **4a**, O: **4b**, S: **4c**) by reaction of diesters **2a**–**c** with (*S*)-valinol.

hand, the acid-catalyzed cyclization of **1** in refluxing acetic anhydride in the presence of H_2SO_4 and subsequent workup gave **2b** in 75% yield, whereas treatment of **1** with Lawessons reagent and subsequent thermal cyclization in refluxing toluene provided a convenient route to **2c** (91% yield).

The preparation of the key intermediates in the subsequent oxazoline synthesis, pyrrole-2,5-bisacetamides **3a**–**c**, was achieved by melting **2a**–**c** with (*S*)-valinol in the presence of catalytic amounts of NaH,[10] giving the reaction products in almost quantitative yield and sufficient purity for the following cyclization step. The synthesis of *i*PrL$_N$H (**4a**) was already reported by the route depicted in Scheme 1.[8] In the same way, conversion of **3b** and **3c** into the bis(oxazolinylmethyl) derivatives *i*PrL$_O$ (**4b**) and *i*PrL$_S$ (**4c**), respectively, was conveniently achieved by reaction with the tetranuclear zinc complex [$Zn_4O(O_2CCF_3)_6$], first employed by Oshima et al. for this purpose.[11]

Reactivity of the Bis(oxazolinylmethyl)pyrroles in Solution: Their Potential to Isomerize

We previously noted that pyrrmebox ligands have the tendency to undergo isomerization by a formal 1,3-H shift when coordinated to palladium(II) or rhodium(I).[7,8] As will be discussed below, similar behaviour may be observed for the nickel complexes reported in this work. Given this general reactive pattern of this class of ligands, a more detailed study of the properties of these protioligands was warranted. To assess the thermodynamic feasibility of such a transformation a DFT study [B3PW91, 6-31g(d) basis set] of *i*PrL$_N$H (**4a**) and its isomeric form *iso*-*i*PrL$_N$H was carried out. The computed minimum structures of **4a** in the gas phase as well as in a solvent phase (chlorobenzene) modelled with the polarizable continuum model (PCM, see Experimental Section) are represented in Figure 1. We note that the three heterocycles of the ligand in the gas phase adopt an arrangement that is closer to C_2 symmetry than that found for the minimum energy structure in the PCM-modelled solution. In the latter, one of the oxazoline rings is twisted out of the approximate planar arrangement of the heterocycles, giving rise to an increased molecular dipole moment that is favoured by the polar environment.

An analogous study was carried out for *iso*-*i*PrL$_N$H in a PCM-modelled solution of chlorobenzene, and the energy of the minimized structure was found to be almost identical to that of *i*PrL$_N$H (**4a**). The computed stabilization 0.6 kcal mol^{-1} is reduced to 0.2 kcal mol^{-1} for the free energy. From a thermodynamic point of view, an equilibrium between *i*PrL$_N$H and *iso*-*i*PrL$_N$H was therefore expected.

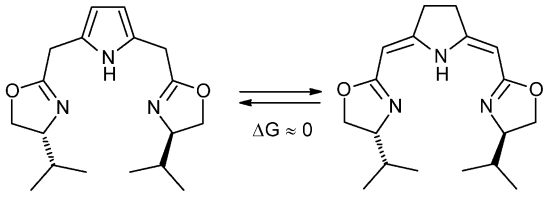

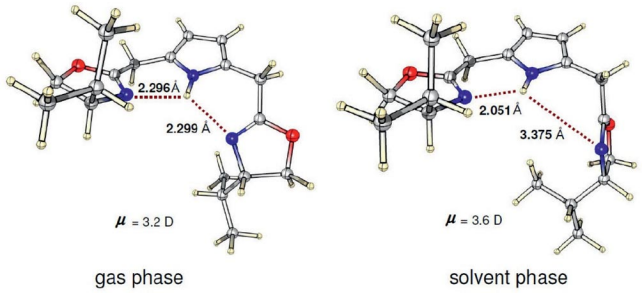

Figure 1. Structural model representing the DFT(B3PW91) optimized geometries of protioligand **4a** in (left) the gas phase and (right) by applying a continuum polarized medium (CPM) phase (chlorobenzene). A significant desymmetrization of **4a** was found when the polar solvent medium was taken into account.

The fact that such an equilibrium was not observed in solution upon heating a sample of *i*PrL$_N$H (**4a**) in chlorobenzene at 80 °C is attributed to the high activation barrier for the orbital symmetry-forbidden 1,3-sigmatropic H-shift.[12]

In order to probe for possible nonconcerted hydrogen transfer by a protolytic route, *i*PrL$_N$H was stirred in MeOD at ambient temperature and under reflux. Neither incorporation of deuterium nor rearrangement was observed under these conditions. However, upon addition of acetic acid (1 equiv.) complete hydrogen/deuterium exchange in the two bridging methylene groups of the ligand was observed (Scheme 2).

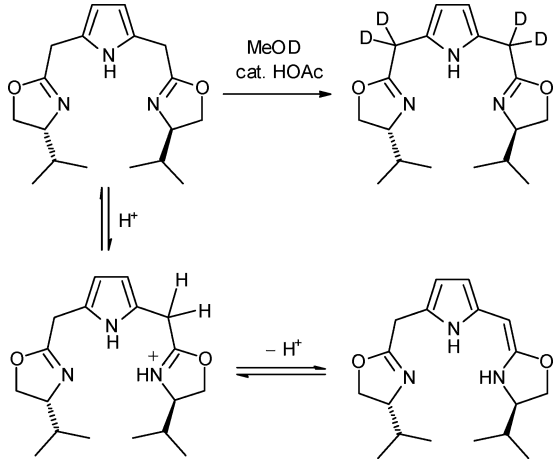

Scheme 2. H/D exchange in the methylene positions of **4a** and a possible enamine/imine tautomerization pathway explaining the selectivity of the process.

The rapid and exclusive incorporation of deuterium in the methylene position and the absence of deuterium incorporation in the pyrrole ring indicated that there must be a kinetically favoured alternative reaction channel. This was thought to be provided by the proton-catalyzed imine/enamine tautomerization indicated in Scheme 2, which involves the oxazoline rings. Such a process would be additionally favoured by the ability of the acetate to bridge the 1,3-C-N unit involved and act both as a proton donor and acceptor. In order to assess the kinetic feasibility the

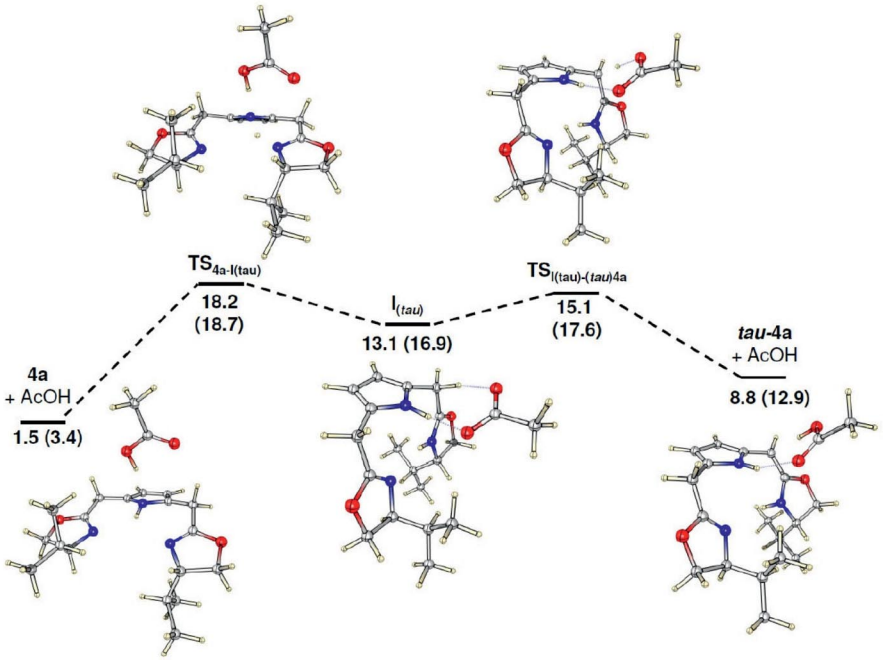

Figure 2. Theoretically modelled reaction pathway for the proton–deuterium exchange in **4a**. Zero-point corrected energies (ΔE_{zp}) and free energies (ΔG) (the latter in parentheses) are given in kcal mol^{-1}.

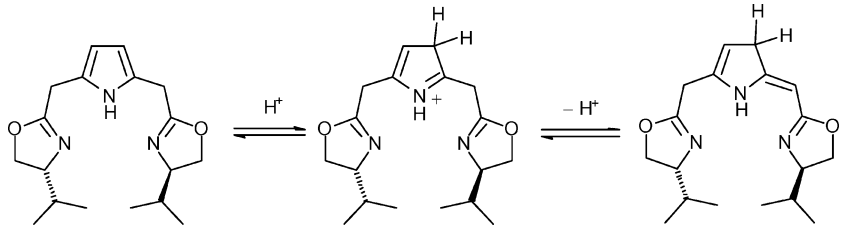

Scheme 3. Nonconcerted 1,3-H shift into the parole ring of **4a** by protonation/deprotonation. This process is associated with a significantly higher activation barrier than the reaction sequence represented in Scheme 2.

complete reaction pathway, the *i*PrL$_N$H–HOAc pair was theoretically modelled in a DFT study. The minimum energy structures of the intermediates as well as the computed structures of the transition states connecting them are depicted in Figure 2.

Starting from the energy minimum adduct between *i*PrL$_N$H and AcOH, in which the acid is associated with N(1) of the pyrrole ring in the ligand, a transition state was found, in which simultaneous protonation of the pyrrole by acetic acid with concomitant proton transfer from the pyrrole to the oxazoline occurs (ΔE_{zp} = 18.2 kcal mol^{-1}; ΔG = 18.7 kcal mol^{-1}). We note that the direct protonation of the oxazoline ring appears to proceed by an energetically disfavoured pathway. The *i*PrL$_N$H$_2^+$/OAc$^-$ ion pair $\mathbf{I}_{(tau)}$ that is formed (ΔE_{zp} = 13.1 kcal mol^{-1}; ΔG = 16.9 kcal mol^{-1}) is geometrically disposed such as to pass through a low activation barrier transition state, in which the proton of the methylene group is abstracted by the acetate (ΔE_{zp} = 2.0 kcal mol^{-1}; ΔG = 0.7 kcal mol^{-1}, with respect to intermediate $\mathbf{I}_{(tau)}$). Finally, the tautomeric form of the oxazoline is obtained as an acetic acid adduct. Liberation of the acetic acid molecule, its proton–deuterium exchange and the subsequent reformation of the thermodynamically favoured starting compound by the corresponding reverse reaction pathway leads to proton–deuterium exchange at the methylene bridges.

The alternative acetate-assisted protolytic 1,3-H shift between the methylene group and the 3-position in the pyrrole ring was also theoretically modelled by using the same DFT tool (Scheme 3; details of this study are provided in the Supporting Information) Such a process would underlie a potential rearrangement of *i*PrL$_N$H → *iso*-*i*PrL$_N$H and was found to proceed through significantly higher activation barriers, which may explain the fact that it has not been observed experimentally.

Synthesis and Structural Characterization of [Bis(oxazolinylmethyl)pyrrolato]nickel(II) Complexes and their Ligand-Based Isomerized Forms

Deprotonation of *i*PrL$_N$H (**4a**) with *t*BuLi at –78 °C and subsequent stirring with $NiCl_2$ yielded the square planar nickel(II) complex **5** as a deep red solid (Scheme 4). Its ana-

lytical data are consistent with its formulation as [Ni(*i*PrL$_N$)Cl], and the ^{1}H and ^{13}C NMR spectral patterns are consistent with a C_2-symmetric molecular species. The pyrrole NH resonance of **4a** has disappeared in **5** and the C*H*Me$_2$ proton resonance is characteristically shifted to lower field (δ =2.71 ppm) relative to that of the corresponding signal of protioligand **4a** (δ =1.72 ppm), indicating the coordination of the pyrrolato unit and two oxazoline rings to the nickel atom.

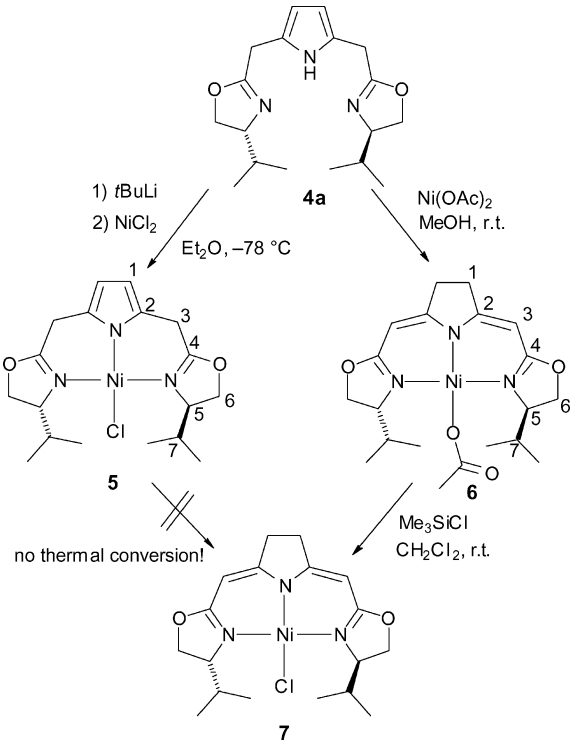

Scheme 4. Synthesis of the nickel(II) complex [Ni(*i*PrL$_N$)Cl] (**5**) and its (ligand-) isomeric form [Ni(*iso*-*i*PrL$_N$)Cl] (**7**) via the acetate complex [Ni(*iso*-*i*PrL$_N$)(OAc)] (**6**).

To establish the structural details of **5**, a single-crystal X-ray structure analysis was carried out. Two views of its molecular structure are depicted in Figure 3 along with the principal bond lengths and angles. The coordination geometry at the nickel centre is almost ideally square planar [N(1)–Ni–N(2) 177.77(7)°, N(3)–Ni–Cl 176.08(6)°; sum of interligand angles 360.06(2)°]. The Ni–N bonds involving the two oxazoline units [Ni–N(1) 1.898(2) Å, Ni–N(2) 1.898(2) Å are slightly longer than Ni–N(3) of the central pyrrolato unit [1.868(2) Å], whereas the interatomic distances within the pyrrole ring are as expected [N(3)–C(5) 1.373(3) Å; C(5)–C(6) 1.376(3) Å; C(6)–C(7) 1.412(3) Å; C(7)–C(8) 1.375(3) Å; C(8)–N(3) 1.373(3) Å].[13]

In order to adapt to the radius of the central atom, the tridentate ligand adopts a helical twist [torsion angles C(5)–C(4)–C(3)–N(1) –40.2(3)° and C(8)–C(9)–C(10)–N(2) –36.9(3)°], which is greater than previously found for the 4d transition metals Rh^{I} and Pd^{II},[7,8] thus reflecting the "contraction" of the binding site. The bond angles at the linking methylene bridges of the meridionally coordinating ligand of C(3)–C(4)–C(5) 110.1(2)° and C(8)–C(9)–C(10) 110.7(2)° are close to the ideal tetrahedral angles and indicate the absence of significant intraligand strain. In attempts to study the potential dynamic exchange between the two helically twisted conformers by low-temperature ^{1}H NMR spectroscopy no line broadening was observed down to –80 °C, indicating rapid exchange, which is consistent with previous observations.[7]

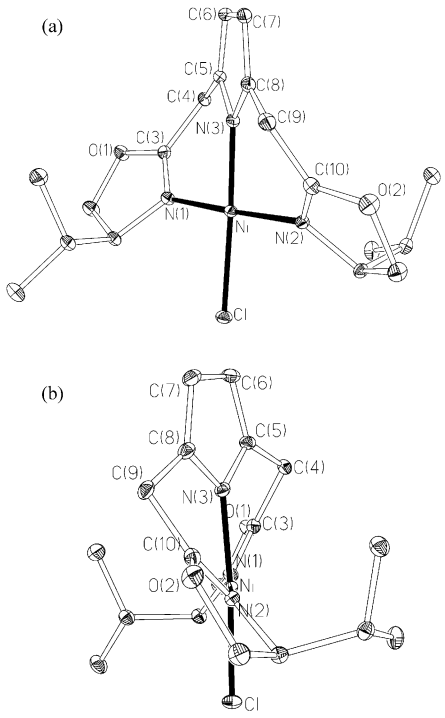

Figure 3. (a) Molecular structure of **5** (hydrogen atoms omitted for clarity; thermal ellipsoids displayed at 30% probability). Selected bond lengths [Å] and angles [°]: Cl–Ni 2.2086(5), N(1)–Ni 1.898(2), N(2)–Ni 1.898(2), N(3)–Ni 1.868(2), N(3)–C(5) 1.373(3), C(5)–C(6) 1.376(3), C(6)–C(7) 1.412(3), C(7)–C(8) 1.375(3), C(8)–N(3) 1.373(3), C(4)–C(5) 1.495(3), C(8)–C(9) 1.493(3), N(2)–Ni–N(1) 177.77(7), N(3)–Ni–Cl 176.08(6), C(3)–C(4)–C(5) 110.2(2), C(8)–C(9)–C(10) 110.7(2), N(1)–Ni–Cl 91.29(5), Cl–Ni–N(2) 90.60(5), N(2)–Ni–N(3) 88.96(7), N(3)–Ni–N(1) 89.24(7), C(8)–C(9)–C(10)–N(2) –36.9(3), C(5)–C(4)–C(3)–N(1) –40.2(3); (b) in-plane view along the axis N(2)–Ni–N(1) illustrating the helical twist of the tridentate ligand.

Upon stirring *i*PrL$_N$H (**4a**) with nickel acetate in methanol, deep red nickel acetato complex **6** bearing the tridentate pincer ligand was obtained (Scheme 4). However, isomerization and concomitant planarization of the ligand occurred in the process, as evident in the ^{1}H and ^{13}C NMR signal patterns. The pyrrole backbone is dearomatized, which is reflected in the chemical shifts of the H(1) protons and the C(1) carbon (Scheme 4), which resonate at 1.42 and 43.6 ppm, respectively, whereas the methylene bridge is converted into a methine fragment CH [δ(^{1}H) = 4.13 ppm, δ(^{13}C) = 85.7 ppm] linked with the central pyrrolidine ring through an exocyclic C=C bond. The isomeric ligand structure, resulting from a formal 1,3-hydrogen shift is planar. In order to establish the details of the molecular structure of [Ni(*iso*-*i*PrL$_N$)(OAc)] (**6**), single-crystal X-ray structure analysis was carried out. There are two independent mole-

cules of **6** in the asymmetric unit. One of them is depicted in Figure 4, the metric parameters of which will be discussed below, and the data of the second molecule, which has a virtually identical geometry, are given in brackets.

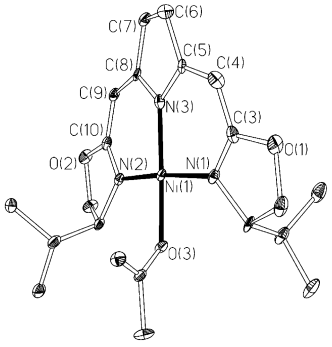

Figure 4. Molecular structure of **6** (hydrogen atoms omitted for clarity; thermal ellipsoids displayed at 30% probability). Only one of the two independent molecules is shown. Selected bond lengths [Å] and angles [°], values given in square brackets refer to the second molecule: Ni(1)–O(3) 1.881(4) [1.876(4)], N(1)–Ni(1) 1.887(5) [1.898(5)], N(2)–Ni(1) 1.897(5) [1.883(5)], N(3)–Ni(1) 1.913(5) [1.895(5)], C(5)–C(6) 1.485(8) [1.495(8)], C(6)–C(7) 1.504(8) [1.510(8)], C(7)–C(8) 1.490(8) [1.490(8)], C(8)–N(3) 1.381(7) [1.358(7)], N(3)–C(5) 1.389(7) [1.388(7)], C(4)–C(5) 1.361(8) [1.357(8)], C(8)–C(9) 1.357(8) [1.359(8)], C(3)–C(4)–C(5) 122.1(6) [123.0(5)], C(8)–C(9)–C(10) 122.7(5) [122.2(5)], N(1)–Ni(1)–N(2) 172.3(2) [175.2(2)], N(3)–Ni(1)–O(3) 178.6(2) [177.2(2)], N(1)–Ni(1)–O(3) 88.8(2) [89.4(2)], O(3)–Ni(1)–N(2) 86.7(2) [86.6(2)], N(2)–Ni(1)–N(3) 92.5(2) [91.4(2)], N(3)–Ni(1)–N(1) 92.2(2) [92.4(2)], C(5)–C(4)–C(3)–N(1) –7.9(9) [–6.0(10)], C(8)–C(9)–C(10)–N(2) 0.2(9) [–4.5(9)].

Similar to complex **5**, [Ni(*iso*-*i*PrL_N)(OAc)] (**6**) has an almost ideal square-planar coordination geometry. The acetate ligand is κ^1-bonded in a *trans* disposition to the central anionic pyrrolidinato ring. The carbon–carbon bond lengths within the pyrrolidinato ring in **6** [C(5)–C(6) 1.485(8) Å, C(6)–C(7) 1.504(8) Å, C(7)–C(8) 1.490(8) Å] are elongated relative to those of **5** and correspond to single bonds, whereas two exocyclic C=C bonds were formed in the rearrangement [C(4)–C(5) 1.361(8) Å, C(8)–C(9) 1.357(8) Å].[14] The helical twist between the pyrrolidine ring and the plane spanned by the ligating atoms has almost disappeared. The relevant torsional angles are C(5)–C(4)–C(3)–N(1) –7.9(9)° and C(8)–C(9)–C(10)–N(2) 0.2(9)°.

Reaction of acetato complex **6** with Me_3SiCl in dichloromethane cleanly gave the corresponding chlorido complex [Ni(*iso*-*i*PrL_N)Cl] (**7**), which is the isomer of compound **5** (Scheme 2). It is notable that it was not possible to induce a rearrangement from **5** into **7** thermally (vide infra), as was readily achieved previously in the conversion of the rhodium(I) complex [Rh(*i*PrL_N)(CO)] to [Rh(*iso*-*i*PrL_N)(CO)], and thus the indirect route via **6** appears to be the only viable preparative method for **7**. Its ^{1}H and ^{13}C NMR spectroscopic data are similar to those of **6**, and the planarized structure was also established by X-ray diffraction. The molecular structure of **7** is depicted in Figure 5 along with selected metric parameters. We note that the planarization of the ligand structure is again reflected in the reduced torsional angles of C(5)–C(4)–C(3)–N(1) –3.8(5)°, C(8)–C(9)–C(10)–N(2) –3.8(4)°.

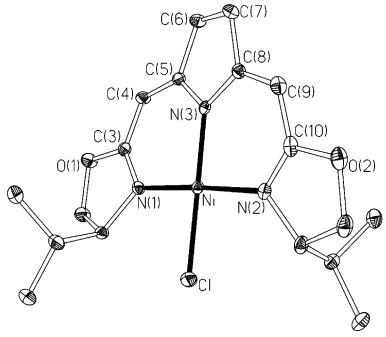

Figure 5. Molecular structure of **7** (hydrogen atoms omitted for clarity; thermal ellipsoids displayed at 30% probability). Selected bond lengths [Å] and angles [°]: Cl–Ni 2.1961(7), N(1)–Ni 1.920(2), N(2)–Ni 1.922(2), N(3)–Ni 1.932(2), C(5)–C(6) 1.514(4), C(6)–C(7) 1.514(4), C(7)–C(8) 1.495(4), C(8)–N(3) 1.366(3), N(3)–C(5) 1.370(3), C(4)–C(5) 1.343(4), C(8)–C(9) 1.354(4), C(3)–C(4)–C(5), 121.3(2), C(8)–C(9)–C(10) 121.3(2), N(3)–Ni–Cl 178.98(7), N(1)–Ni–N(2) 176.21(10), N(1)–Ni–Cl 88.68(7), Cl–Ni–N(2) 88.44(7), N(2)–Ni–N(3) 91.27(9), N(3)–Ni–N(1) 91.65(9), C(5)–C(4)–C(3)–N(1) –3.8(5), C(8)–C(9)–C(10)–N(2) –3.8(4).

Theoretical Modelling of the Ligand Isomerization in the Nickel(II) Complexes

The characterization of chloridonickel(II) complexes **5** and **7** raised the question of their relative free energies. Furthermore, it was of interest to find an explanation for the facile ligand rearrangement from {*i*PrL_N}$^-$ to {*iso*-*i*PrL_N}$^-$ in the synthesis of acetatonickel complex **6**. To address the former question, a DFT study [B3PW91, 6-31g(d) for C, N, O, H, Cl and an effective small core potential basis set for Ni; see the Experimental Section] of both chloridonickel complexes **5** and **7** was carried out. All the metric parameters were found to agree well with those determined by X-ray diffraction, and the experimental and computed data are compared in Table 1.

Table 1. Comparison of selected experimentally determined and computed structural parameters of compounds **5** and **7**.

Structural parameter	**5**		**7**	
	X-ray	DFT	X-ray	DFT
d(Ni–Cl) [Å]	2.209	2.220	2.196	2.222
d[Ni–N(1)] [Å]	1.898	1.915	1.922	1.921
d[Ni–N(2)] [Å]	1.898	1.911	1.920	1.921
d[Ni–N(3)] [Å]	1.868	1.874	1.932	1.929
d[C(5)–C(4)–C(3)–N(1)] [°]	–40.2	–38.4	–3.8	–8.5
d[C(8)–C(9)–C(10)–N(2)] [°]	–36.9	–35.8	–3.8	–8.5

Whereas the isomerized form of the protioligand *iso*-*i*PrL_NH was essentially isoenergetic with *i*PrL_NH, the nickel complex [Ni(*iso*-*i*PrL_N)Cl] (**7**) was found to be stabilized in comparison to **5** by –9.3 kcal mol^{-1} (ΔG = –9.8 kcal mol^{-1}). The observed resistance of **5** with respect to a thermally induced isomerization to **7** must therefore be due to the high activation barrier associated with the 1,3-sigmatropic

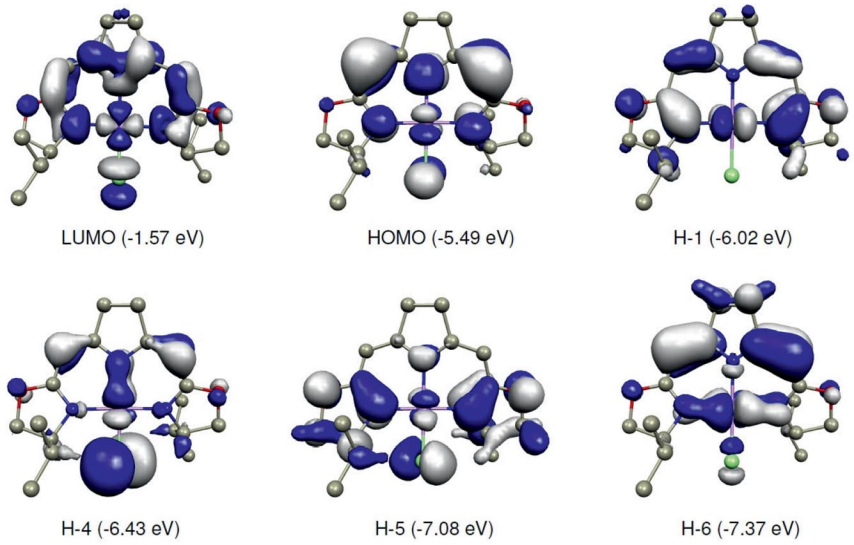

Figure 6. The frontier orbitals in complex **7** illustrating the π conjugation within the ligand system (HOMO, HOMO-1, HOMO-5, HOMO-6) and the π-bonding interaction with the metal (HOMO-4).

H-shift. The stabilization of **7** with respect to **5** may be attributed to the formation of a conjugated π system within the rearranged ligand, which interacts with the metal centre. This aspect is illustrated by the Kohn Sham frontier orbitals of computed complex **7** represented in Figure 6. Whereas the conjugation between the double bonds within the ligand is represented by the structure of the HOMO, HOMO-1, HOMO-6 and HOMO-7, the π-bonding interaction is particularly evident in the HOMO-4 frontier orbital.

To address the question of the possible role of the acetate in the rearrangement of the coordinated ligand $\{iso\text{-}i\mathrm{PrL_N}\}^-$ in the formation **6**, the interaction of complex **5** with a molecule of acetic acid (liberated in the generation of **6** from $i\mathrm{PrL_N H}$ and nickel acetate) was theoretically modelled by DFT. In this study, the resulting minimum energy reaction pathway involving a possible acetic acid catalyzed rearrangement of the coordinated ligand was computed and is represented in Figure 7. An analogous computational study was carried out for the transformation of the experimentally not observed complex [Ni($i\mathrm{PrL_N}$)(OAc)] into [Ni(*iso*-$i\mathrm{PrL_N}$)(OAc)] (**6**). The free-energy profiles for both transformations were found to be almost identical, and the details for the latter are given in the Supporting Information.

Starting from a weakly bonded adduct between AcOH and the C3/4-position of the coordinated ligand in **5** (ΔE_{zp} = 0.0 kcal mol^{-1}; ΔG = 0.0 kcal mol^{-1}), a transition state was found in which a proton transfer from the methylene group to the bridging acetate occurs simultaneously with the protonation of the C3/4-position of pyrrole ($\mathbf{TS_{5(Cl)\text{-}I1(OAc)}}$: ΔE_{zp} = 19.4 kcal mol^{-1}; ΔG = 21.0 kcal mol^{-1}). Intermediate $\mathbf{I_1}$ generated in this process rearranges into an isomeric ad-

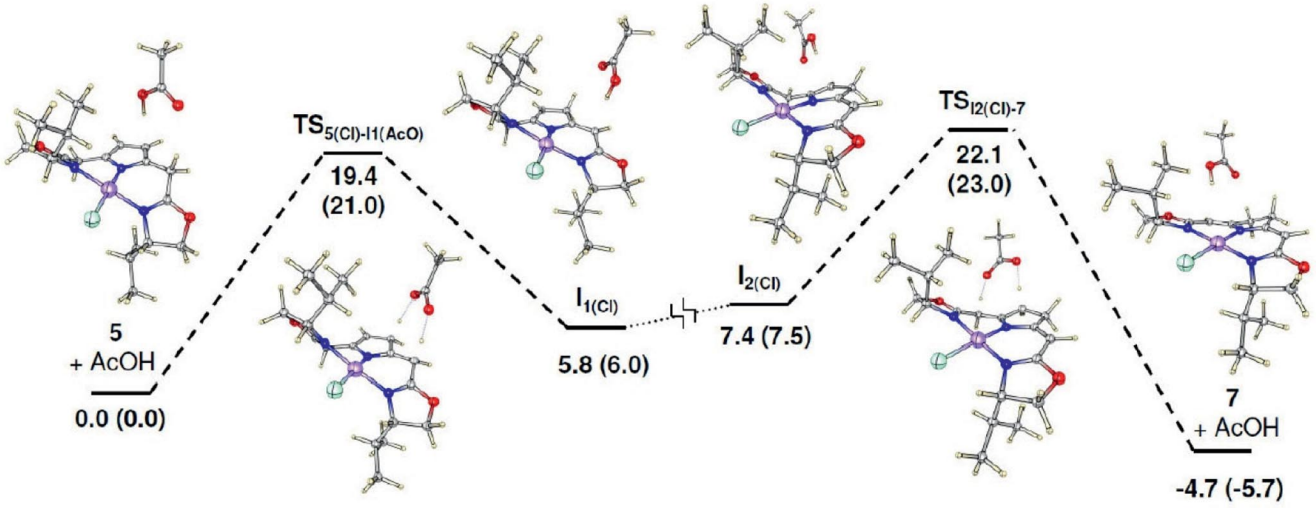

Figure 7. Computed HOAc-mediated rearrangement pathway for the transformation of **5**(HOAc) into **7**(HOAc). Zero-point corrected energies (ΔE_{zp}) and free energies (ΔG) (the latter in parentheses) are given in kcal mol^{-1}.

duct with acetic acid $\mathbf{I_{2(Cl)}}$ (ΔE_{zp} = 7.4 kcal mol^{-1}; ΔG = 7.5 kcal mol^{-1}), in which the associated acetic acid is geometrically disposed to allow a similar concerted protonation/deprotonation, passing through a low-barrier transition state $\mathbf{TS_{I2(Cl)-7}}$, leading to the rearrangement complex.

This mechanistic proposal is supported by the observed rearrangement of **5** into **7** upon exposure of the chloridonickel complex to acetic acid. Further experimental evidence for this reaction pathway in the generation of acetato complex **6** was obtained by reaction of N-deuterated protioligand **4a[D]** with nickel acetate in dmf. Incorporation of deuterium in the 1-position of the rearranged ligand (Scheme 4) is consistent with the intermediate generation of deuterated acetic acid and subsequent proton transfer to the pyrrole ring, as postulated above. Small amounts of deuterium in the bridging CH position (at C3) indicated that some deuterium exchange had taken place with the protioligand itself prior to its coordination, according to the mechanism represented in Scheme 2.

It is interesting to compare this mechanistic scenario with that discussed above for the deuterium exchange observed for the protioligand. Upon coordination of the ligand to a metal centre, the formation of N-protonated oxazoline intermediates is not possible anymore. Therefore, this low-activation process, which appears to operate in the protioligand and leaves the pyrrole ring intact, is barred. In contrast, proton transfer with the C3/4-position of the pyrrole ring remains a viable reaction channel and the ligation of pyrrmebox to the metal centre appears to lower the activation barrier for this process. The reaction is additionally favoured by the thermodynamic driving force ($\Delta G < 0$) associated with it in the transformation of **5** → **7**.

Synthesis and Structural Characterization of a [Bis(oxazolinylmethyl)furan]chromium(III) Complex

Both furans and thiophenes have proved to be only weakly κ*O*- or κ*S*-coordinating ligands, and the number of structurally characterized complexes bearing these ligating motifs remains limited. In the case of tridentate bisoxazolines containing the dibenzofuran (**Ib**) and dibenzothiophene (**Ic**) backbones, the rigidity of the ligand structures supported their coordination through all three heterocyclic units. In contrast, for both ligands *i*PrL$_O$ (**4b**) and *i*PrL$_S$ (**4c**), the heterocycles are connected by the highly flexible methylene bridges, and this meridional tricoordination is much less favoured. This is thought to be the reason for the inability of the thiophene derivative *i*PrL$_S$ (**4c**) to coordinate to nickel(II) upon reaction with either $NiCl_2$, $Ni(ClO_4)_2$ or $[Ni(NH_3)_6]^{2+}$ salts in a wide range of solvent systems. Furthermore, whereas *i*PrL$_O$ (**4b**) appeared to react with nickel(II) salts in solution, the resulting complexes proved to be highly labile and could not be isolated as well-defined materials. In view of Nakada's previous studies of the Nozaki–Hiyama allylation with chromium(III) complexes bearing chiral pincers,[4] we investigated the coordination capability of **4b** and **4c** towards Cr^{III}.

Reaction of *i*PrL$_O$ (**4b**) with $[CrCl_3(thf)_3]$ in thf gave the yellow-green complex $[CrCl_3(i\text{PrL}_O)]$ (**8**), whereas no complexation occurred with the analogous thiophene-derived bisoxazoline (Scheme 5). Both analytical and mass spectrometric data were compatible with the formulation of complex **8**, the structural details of which were established by X-ray diffraction. Its molecular structure is depicted in Figure 8 along with selected bond lengths and angles.

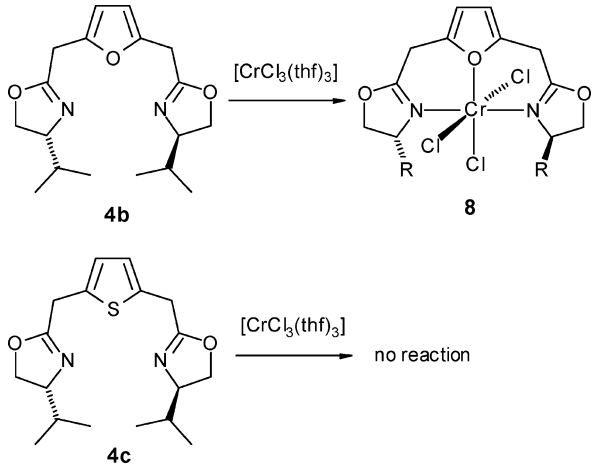

Scheme 5. Synthesis of the chromium(III) complex $[Cr(i\text{PrL}_O)Cl_3]$ (**5**), whilst no complexation is observed with *i*PrL$_S$ (**4c**).

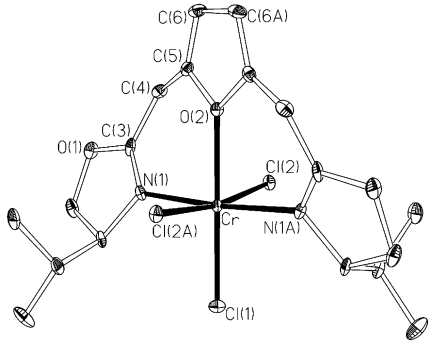

Figure 8. Molecular structure of **8** (hydrogen atoms omitted for clarity; thermal ellipsoids displayed at 25% probability). Selected bond lengths [Å] and angles [°]: N(1)–Cr 2.066(4), O(2)–Cr 2.112(4), Cl(1)–Cr 2.256(2), Cl(2)–Cr 2.325(1), O(2)–C(5) 1.384(5), C(5)–C(6) 1.346(7), C(6)–C(6A) 1.398(10), C(4)–C(5) 1.484(6), C(3)–C(4)–C(5) 118.4(4), Cl(1)–Cr–Cl(2) 94.81(3), Cl(2)–Cr–O(2) 85.19(3), Cl(1)–Cr–N(1) 92.67(11), N(1)–Cr–O(2) 87.33(11), N(1A)–Cr–Cl(2) 90.61(10), Cl(2)–Cr–N(1) 88.95(10), Cl(2)–Cr–Cl(2A) 170.39(7), O(2)–Cr–Cl(1) 180.00(5), N(1A)–Cr–N(1) 174.7(2), N(1)–C(3)–C(4)–C(5) –30.8(7).

In the crystal structure, the molecular twofold axis coincides with a crystallographic C_2 symmetry axis. The bis(oxazolinylmethyl)furan ligand did not isomerize upon coordination to chromium and therefore adopts the helically twisted conformation referred to above [N(1)–C(3)–C(4)–C(5) –30.8(7)°]. We also note some strain at the bridging methylene units, as manifested in the angle C(3)–C(4)–C(5) of 118.4(4)°, which is significantly greater than expected for sp^3 carbon atoms. The coordination geometry around the chromium centre is slightly distorted octahedral. The ligat-

ing atoms N(1), O(2), N(1A) and Cl(1) [sum of interligand angles 360.0(6)°] and Cl(1), Cl(2), O(3) and Cl(2A) [sum of interligand angles 360.0(6)°] lie on two mutually orthogonal planes of the octahedron. The interatomic distances within the planar furan ring are as expected [O(2)–C(5) 1.384(5) Å, C(5)–C(6) 1.346(7) Å, C(6)–C(6A) 1.398(10) Å].[13]

Conclusions

In this work, we have presented a mechanistic rationale for the intraligand rearrangement observed for transition-metal complexes in the presence of a carboxylate as a proton transfer relay. Both the H/D exchange in the free protioligand and the formal 1,3-H shifts observed for the metal complexes are satisfactorily explained within the framework of this model. However, such rearrangements have also been observed in the absence of an acid[8] and inter alia in the presence of palladium precursor complexes.[7] This indicates that there may be other mechanistic pathways that allow the forbidden concerted rearrangement to be circumvented.

We have reported the synthesis of the furan and thiophene analogues of pyrrmebox, a first assessment of their complexation capability as well as their apparent limitations as ligands for late-transition metals. Further work to clarify this point is underway in our laboratory.

Experimental Section

General: All manipulations of air- and moisture-sensitive species were performed under an atmosphere of argon by using standard Schlenk and glove box techniques. Solvents were predried with molecular sieves and dried with Na/K alloy (diethyl ether), Na (toluene) or K (thf, hexane), distilled and stored over potassium mirrors (hexane, diethyl ether and toluene) in Teflon-valved ampoules. Deuterated solvents were dried with K ([D_6]benzene, [D_8]toluene) or CaH_2 ($CDCl_3$, CD_2Cl_2), vacuum distilled and stored under an atmosphere of argon in Teflon-valved ampoules. Samples for NMR spectroscopy were prepared under an atmosphere of argon in 5 mm Wilmad tubes equipped with J. Young Teflon valves. NMR spectra were recorded with Bruker Avance II 400 or Bruker Avance III 600 NMR spectrometers. NMR spectra are quoted in ppm and were referenced internally relative to the residual protio solvent (^1H) or solvent (^{13}C) resonances. Where necessary, NMR assignments were confirmed by the use of 2D ^1H–^1H or ^1H–^{13}C correlation experiments. Microanalyses were performed by the analytical services in the chemistry departments of the University of Heidelberg. IR spectra were recorded with a Varian 3100 Exalibur spectrometer as KBr plates. Compounds **1**, **2a**, **3a** and **4a** were prepared as reported previously.[8]

Modified Synthetic Procedure for Furan-2,5-diethyl Acetate (2b): To a solution of 3,6-dioxo-1,8-octanediethyl acetate (**1**; 2.0 g, 7.74 mmol) dissolved in acetic anhydride (20 mL) was added concentrated H_2SO_4 (0.5 mL), and the mixture was heated at reflux for 3 h. During the course of the reaction the yellow solution gradually turned brown. The reaction mixture was then poured onto crushed ice (150 g). After neutralization with a saturated aqueous solution of $NaHCO_3$, the resulting mixture was extracted with dichloromethane (3 × 200 mL). The combine organic extract was dried with Na_2SO_4 and filtered, and the solvents were evaporated to dryness. The crude product was purified by column chromatography on silica (hexane/EtOAc, 9:1; R_f = 0.49). The pure product was obtained as a light yellow oil in 75% yield. The spectroscopic and analytical data were identical to those reported by Simone et al.[9a]

Modified Synthetic Procedure for Thiophene-2,5-diethyl Acetate (2c): A mixture of 3,6-dioxo-1,8-octanediethyl acetate (**1**; 1.0 g, 3.87 mmol) and Lawesson's reagent (1.9 g, 4.65 mmol) was heated at reflux in toluene (40 mL) for 4 h. After removal of the solvent in vacuo, the crude product was purified by column chromatography on silica (hexane/EtOAc, 9:1; R_f = 0.46). The pure product was obtained as a yellow oil in 91% yield. The spectroscopic and analytical data were identical to those reported by Flitsch et al.[9b]

2,5-Bis({[*N*-1-hydroxy-2-(*S*)-isopropylethyl]acetamido}methyl)furan (3b): Compound **2b** (1.5 g, 6.24 mmol) and L-valinol (1.35 g, 13.11 mmol) were weighed into a large Schlenk tube, which was evacuated several times and then placed under an argon atmosphere. The reaction mixture was then melted in an oil bath, which had been preheated to 120 °C, and then NaH (suspended in paraffin, 1 g) was added. The reaction mixture was stirred under a dynamic vacuum for 2 h, until the melt had completely solidified. After cooling to ambient temperature, the crude product was purified by column chromatography on silica (dichloromethane/methanol, 89:11; R_f = 0.18). The product was obtained as a slightly hygroscopic, light yellow solid in 46% yield. ^1H NMR (600.13 MHz, $CDCl_3$, 296 K): δ = 6.25 (d, ^3J = 8.9 Hz, 2 H, N-*H*), 6.16 (s, 2 H, H^1), 3.75–3.68 (m, 2 H, H^5), 3.66–3.54 (m, 4 H, H^6), 3.57 (s, 4 H, H^3), 1.82 (dsept., ^3J = 6.8 Hz, 2 H, H^7), 1.25 (br., 2 H, O-*H*), 0.92 (d, ^3J = 6.8 Hz, 6 H, CH*Me*Me), 0.88 (d, ^3J = 6.8 Hz, 6 H, CHMe*Me*) ppm. $^{13}C\{^1H\}$ NMR (151 MHz, $CDCl_3$, 296 K): δ = 169.7 (C^4), 148.8 (C^2), 109.7 (C^1), 63.1 (C^6), 57.2 (C^5), 36.3 (C^3), 29.3 (C^7), 19.6 (C^8), 19.1 (C^9) ppm. IR (KBr plates): $\tilde{\nu}$ = 3468 (m, br.), 3308 (s, br.), 2960 (m, br.), 1659 (s), 1623 (s), 1551 (s), 1472 (w), 1397 (w), 1359 (m), 1197 (w), 1149 (w), 1063 (m), 1016 (m), 984 (w), 960 (w), 795 (m), 741 (w), 697 (w), 573 (w), 504 (w) cm^{-1}. MS (FAB): *m*/*z* (%) = 377 (75) $[M + Na]^+$, 355 (100) $[M + H]^+$. HRMS (FAB+): calcd. for $C_{18}H_{31}N_2O_5^+$ 355.2227; found 355.2241. $C_{18}H_{30}N_2O_5$ (354.44): calcd. C 61.0, H 8.5, N 7.9; found C 61.1, H 8.7, N 7.8.

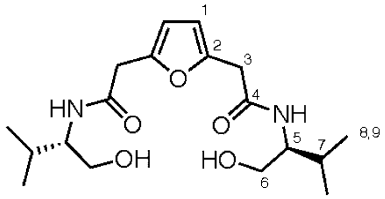

2,5-Bis({[*N*-1-hydroxy-2-(*S*)-isopropylethyl]acetamido}methyl)thiophene (3c): Compound **2c** (769 mg, 3 mmol) und L-valinol (928 mg, 9 mmol) were weighed into a large Schlenk tube, which was evacuated several times and then placed under an argon atmosphere. The reaction mixture was then melted in an oil bath, which had been preheated to 120 °C, and then NaH (suspended in paraffin, 1 g) was added. The reaction mixture was stirred under a dynamic vacuum for 2 h, until the melt had completely solidified. After cooling to ambient temperature, the crude product was purified by column chromatography on silica (dichloromethane/methanol, 89:11; R_f = 0.15). The product was obtained as a slightly hygroscopic, light yellow solid in 50% yield. ^1H NMR (600.13 MHz, $CDCl_3$, 296 K): δ = 6.84 (s, 2 H, H^1), 5.90 (br., 2 H, N-*H*), 3.75 (s, 4 H, H^3), 3.72–3.60 (m, 6 H, H^5, H^6), 2.79 (br., 2 H, O-*H*), 1.86–1.80 (sept., 2 H, H^7), 0.92 (d, ^3J = 6.8 Hz, 6 H, CH*Me*Me), 0.87 (d, ^3J = 6.8 Hz, 6 H, CHMe*Me*) ppm. $^{13}C\{^1H\}$ NMR (151 MHz, $CDCl_3$, 296 K): δ = 170.6 (C^4), 136.8 (C^2), 127.8 (C^1), 63.8 (C^6), 57.4 (C^5), 38.1 (C^3),

29.1 (C^7), 19.7 & 19.0 (C^8, C^9) ppm. IR (KBr plates): $\tilde{\nu}$ = 3293 (s, br.), 2962 (s), 1659 (s), 1613 (s), 1551 (s), 1471 (m), 1368 (m), 1245 (m), 1193 (w), 1150 (w), 1061 (m), 1126 (m), 979 (w), 925 (w), 778 (w), 719 (w), 679 (w), 578 (m), 515 (w) cm^{-1}. MS (FAB): *m/z* (%) = 371 (100) $[M + H]^+$. HRMS (FAB+): calcd. for $C_{18}H_{31}N_2O_4S^+$ 371.1999; found 371.1977. $C_{18}H_{30}N_2O_4S$ (370.51): calcd. C 58.4, H 8.2, N 7.5; found 58.4, H 8.1, N 7.4.

2,5-Bis{[(4*S*)-4-isopropyloxazolinyl]methyl}furan (*i*PrL$_O$H) (4b): A solution of compound **3b** (500 mg, 1.35 mmol) and $Zn_4(OCOCF_3)_6O$ (32 mg, 0.034 mmol) in dry chlorobenzene (30 mL) was heated at refluxed under an argon atmosphere for 18 h. After removal of the solvent in vacuo, the crude product was purified by column chromatography on silica (EtOAc/hexane/Et_3N, 62:33:5; R_f = 0.32). The product was obtained as a slightly hygroscopic yellow oil in 93% yield. ^1H NMR (600.13 MHz, $CDCl_3$, 296 K): δ = 6.12 (s, 2 H, H^1), 4.25 (dd, ^3J = 9.5, 8.2 Hz, 2 H, H^6), 4.03–3.89 (m, 4 H, H^6, H^5), 3.63 (s, 4 H, H^3), 1.75 (sept, ^3J = 6.6 Hz, 2 H, H^7), 0.95 (d, ^3J = 6.8 Hz, 6 H, CH*Me*Me), 0.87 (d, ^3J = 6.8 Hz, 6 H, CHMe*Me*) ppm. $^{13}C\{^1H\}$ NMR (151 MHz, $CDCl_3$, 296 K): δ = 163.5 (C^4), 148.2 (C^2), 108.4 (C^1), 72.2 (C^5), 70.5 (C^6), 32.6 (C^7), 28.0 (C^3), 18.8 & 18.2 (C^8, C^9) ppm. IR (KBr): $\tilde{\nu}$ = 2964 (m), 1669 (s), 1519 (m), 1471 (w), 1369 (w), 1176 (w), 1017 (m), 984 (m), 895 (m) cm^{-1}. MS (FAB): *m/z* (%)= 319 (100) $[M + H]^+$. HRMS (FAB+): calcd. for $C_{18}H_{27}N_2O_3^+$ 319.2016; found 319.2008. $C_{18}H_{26}N_2O_3$ (318.41): calcd. C 67.9, H 8.2, N 8.8; found C 67.8, H 8.3, N 8.6.

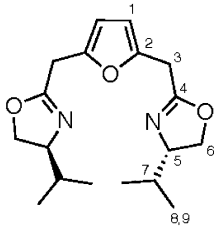

2,5-Bis{[(4*S*)-4-isopropyloxazolinyl]methyl}thiophene (*i*PrL$_S$H) (4c): A solution of compound **3c** (500 mg, 1.35 mmol) and $Zn_4(OCOCF_3)_6O$ (32 mg, 0.034 mmol) in dry chlorobenzene (30 mL) was heated at reflux under an argon atmosphere for 18 h. After removal of the solvent in vacuo, the crude product was purified by column chromatography on silica (EtOAc/hexane/Et_3N, 62:33:5; R_f = 0.31). The product was obtained as a slightly hygroscopic yellow oil in 90% yield. ^1H NMR (399.89 MHz, $CDCl_3$, 296 K): δ = 6.80 (s, 2 H, H^1), 4.25 (dd, ^3J = 9.2, 8.0 Hz, 2 H, H^6), 4.03–3.94 (m, 4 H, H^6, H^5), 3.80 (s, 4 H, H^3), 1.80 (sept., ^3J = 6.6 Hz, 2 H, H^7), 1.00 (d, ^3J = 6.8 Hz, 6 H, CH*Me*Me), 0.92 (d, ^3J = 6.8 Hz, 6 H, CHMe*Me*) ppm. $^{13}C\{^1H\}$ NMR (100 MHz, $CDCl_3$, 296 K): δ = 164.7 (C^4), 136.3 (C^2), 126.3 (C^1), 72.2 (C^5), 70.5 (C^6), 32.6 (C^7), 29.5 (C^3), 18.8 (C^8), 18.2 (C^9) ppm. IR (CH_2Cl_2): $\tilde{\nu}$ = 2964 (m), 1768 (s), 1516 (m), 1422 (w), 1174 (w), 982 (m), 894 (m) cm^{-1}. MS (FAB): *m/z* (%) = 335 (100) $[M + H]^+$. HRMS (FAB+): calcd. for $C_{18}H_{27}N_2O_2S^+$ 335.1788; found 335.1759. $C_{18}H_{26}N_2O_2S\cdot 2/3H_2O$ (346.49): calcd. C 62.4, H 7.9, N 7.8; found C 62.4, H 7.7, N 8.1.

(κ^3-N,N,N-2,5-Bis{[(4S)-4-isopropyloxazolinyl]methyl}pyrrolido)-chloridonickel(II) (5): The protioligand iPrL$_N$H (**2a**; 200 mg, 0.63 mmol) was dissolved in diethyl ether (20 mL) and then metallated at –78 °C by the slow addition of tert-buthyllithium (1.5 M in hexane, 0.42 mL, 0.63 mmol). After complete addition, the reaction mixture was stirred at –78 °C for another 30 min and then a solution of $NiCl_2$ in dimethyl formamide, which had been precooled to –78 °C, was added through a cannula. The reaction mixture was warmed to ambient temperature and stirred for 45 min. After removal of the solvents under vacuum, the residue was dissolved in dichloromethane and filtered. The solvent was evaporated, and the remaining solid was washed with cold pentane. The dark-orange product was recrystallized from a mixture of dichloromethane/hexane (1:1) to give the nickel complex as an analytically pure microcrystalline solid in 75% yield. ^1H NMR (399.89 MHz, $CDCl_3$, 296 K): δ = 5.76 (s, 2 H, H^1), 4.23–4.08 (m, 8 H, H^5, H^6, $H^{6'}$, H^{3A}), 3.48 (AB system, J_{AB} = 18.3 Hz, 2 H, H^{3B}), 2.71 (m, 2 H, H^7), 1.07 (d, ^3J = 6.9 Hz, 6 H, CHMeMe), 0.85 (d, ^3J = 6.9 Hz, 6 H, CHMeMe) ppm. $^{13}C\{^1H\}$ NMR (100 MHz, $CDCl_3$, 296 K): δ = 169.9 (C^4), 125.9 (C^2), 105.3 (C^1), 70.0 (C^6), 66.9 (C^5), 30.9 (C^7), 28.2 (C^3), 18.8 (CHMeMe), 15.7 (CHMeMe) ppm. IR (KBr): $\tilde{\nu}$ = 1960 (m, br.), 1643 (s), 1539 (w), 1478 (m), 1422 (m), 1404 (m), 1317 (w), 1284 (w), 1236 (s), 1149 (w), 1118 (w), 1056 (w), 1001 (m), 949 (m), 917 (w), 789 (m), 735 (m), 643 (w), 611 (w), 425 (m) cm^{-1}. MS EI: m/z = 409 (22) $[M]^+$, 473 (100) $[M – Cl]^+$. HRMS (EI): calcd. for $C_{18}H_{26}{}^{37}ClN_3{}^{58}NiO_2$ 411.1038; found 411.1042. HRMS (EI): calcd. for $C_{18}H_{26}{}^{35}ClN_3{}^{58}NiO_2$ 409.1067; found 409.1035. $C_{18}H_{26}ClN_3NiO_2$ (410.56): calcd. C 52.5, H 6.4, N 10.2; found C 52.5, H 6.3, N 10.0.

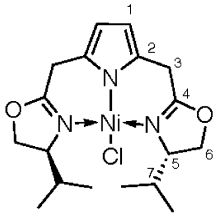

(κ^3-*N*,*N*,*N*-2,5-Bis{[(4*S*)-4-isopropyloxazolinylidene]methyl}pyrrolidinido)acetatonickel(II) (6): The protioligand *i*PrL$_N$H (**2a**; 300 mg, 0.95 mmol) and $Ni(OAC)_2\cdot 4H_2O$ (470 mg, 1.89 mmol) were each dissolved in methanol (15 mL). The ligand solution was added with a cannula to the solution of the metal salt over a period of 10 min. After stirring the reaction mixture for 18 h, the solvent was removed in vacuo, the residue was redissolved in dichloromethane and filtered and the crude reaction product, isolated after evaporation of the filtrate to dryness, was recrystallized from dichloromethane/hexane (1:1) to yield the nickel complex as a microcrystalline red solid in 81% yield. ^1H NMR (399.89 MHz, $CDCl_3$, 296 K): δ = 4.54 (br. s, 2 H, H^3), 4.24 (d, *J* = 6.5 Hz 2 H, H^6), 4.09 (m, 4 H, H^5 + H^6), 2.45 (br. s, 6 H, H^7 + H^1), 2.27 (s, 3 H, COO*Me*), 0.89 (d, *J* = 7.2 Hz, 6 H, CH*MeMe*), 0.76 (d, *J* = 7.2 Hz, 6 H, CH*MeMe*) ppm. $^{13}C\{^1H\}$ NMR (100 MHz, $CDCl_3$, 296 K): δ = 174.3 (C^2), 166.74 (C^4), 159.1 (*C*OOMe), 85.71 (C^3), 75.5 (C^5), 72.5 (C^6), 43.6 (C^1), 33.1 (C^7, COO*Me*), 19.5 (CH*Me*Me), 14.7 (CHMe*Me*) ppm. IR (KBr): $\tilde{\nu}$ = 2960 (w, br.), 1616 (s), 1595 (s), 1544 (s), 1437 (w), 1371 (w), 1318 (m), 1296 (w), 1258 (m), 1232 (s), 1072 (w), 1021 (m), 961 (w), 756 (w), 681 (w), 414 (w) cm^{-1}. MS (EI): *m/z* (%) = 433 (8) $[M]^+$, 373 (100) $[M – OAc]^+$, 331 (13) $[M – OAc – iPr]^+$. HRMS (EI): calcd. for $C_{20}H_{29}N_3{}^{58}NiO_4$ 433.1512; found 433.1521. $C_{20}H_{29}N_3NiO_4\cdot CH_2Cl_2$ (519.09): calcd. C 48.5, H 6.0, N 8.1; found C 48.0, H 6.5, N 8.2.

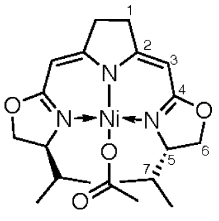

(κ^3-*N*,*N*,*N*-2,5-Bis{[(4*S*)-4-isopropyloxazolinyl]methylidene}pyrrolidinido)chloridonickel(II) (7): To a solution of complex **6** (200 mg, 0.46 mmol) dissolved in dichloromethane (15 mL) was added a solution of Me_3SiCl (59 µL, 50.2 mg, 0.46 mmol) in dichlo-

romethane (5 mL). After stirring for 1 h, the solvent was removed in vacuo and the residue was washed with hexane to give the analytically pure product as a green, air-stable solid in 95% yield. ^{1}H NMR (399.89 MHz, $CDCl_3$, 296 K): δ = 5.84 (br. d, ^3J = 9.0 Hz, 2 H, H^5), 4.19 (dd, J = 8.7, 2.8 Hz, 2 H, H^6), 4.01 (t, J = 8.7 Hz, 2 H, H^6), 3.89 (s, 2 H, H^3), 2.84–2.72 (m, 2 H, H^7), 2.23–2.04 (m, 4 H, H^1), 1.19 (d, ^3J = 6.9 Hz, 6 H, CH*Me*Me), 0.83 (d, ^3J = 6.9 Hz, 6 H, CHMe*Me*) ppm. ^{13}C{^{1}H} NMR (100 MHz, $CDCl_3$, 296 K): δ = 170.9 (C^2), 156.7 (C^4), 87.6 (C^3), 76.1 (C^5), 71.7 (C^6), 33.5 (C^7), 20.6 (C^1), 15.4 (CH*Me*Me), 1.2 (CHMe*Me*) ppm. IR (KBr): $\tilde{\nu}$ = 2867 (m, br.), 1669 (m), 1615 (s), 1589 (s), 1546 (s), 1487 (w), 1464 (w), 1432 (w), 1366 (w), 1317 (w), 1296 (m), 1260 (s), 1230 (s), 1174 (w), 1158 (w), 1097 (m), 1022 (s), 958 (w), 865 (m), 799 (s), 752 (w), 707 (w), 488 (w) cm^{-1}. MS (EI): *m*/*z* (%) = 409 (57) [M]$^+$, 373 (100) [M – Cl]$^+$, 331 (20) [M – Cl – *i*Pr]$^+$. HRMS (EI): calcd. for $C_{18}H_{26}{}^{37}ClN_3{}^{58}NiO_2$ 411.1038; found 411.1046. HRMS (EI): calcd. for $C_{18}H_{26}{}^{35}ClN_3{}^{58}NiO_2$ 409.1067; found 409.1045. $C_{18}H_{26}ClN_3NiO_2$ (410.56): calcd. C 52.7, H 6.4, N 10.2; found C 52.2, H 6.3, N 10.0.

(κ^3-*N*,*O*,*N*-2,5-Bis{[(4*S*)-4-isopropyloxazolinyl]methyl}pyrrolido)trichloridochromium(III) (8): The protioligand *i*PrL$_O$H (**4b**; 300 mg, 0.95 mmol) and [$CrCl_3$(thf$_3$)] (356 mg, 0.95 mmol) were each dissolved in thf (15 mL). The ligand solution was then added with a cannula to the solution of the metal salt over a period of 10 min. After stirring for 2 h, the colour of the reaction mixture had changed from purple to yellow-green. After removal of the solvent in vacuo, the analytically pure product was isolated as a green, moisture-sensitive solid in 96% yield. IR (KBr): $\tilde{\nu}$ = 2932 (m, br.), 1650 (s), 1583 (w), 1485 (m), 1421 (m), 1375 (s), 1323 (w), 1276 (m), 1247 (m), 1224 (s), 1118 (w), 1007 (m), 972 (s), 953 (m), 901 (w), 828 (m), 773 (w), 740 (m), 698 (w), 622 (w), 578 (w) cm^{-1}. MS (EI): *m*/*z* (%) = 475 (1.2) [M]$^+$, 440 (51) [M – Cl]$^+$, 405 (34) [M – Cl – Cl]$^+$, 362 (10) [M – Cl – Cl – *i*Pr]$^+$, 362 (36) [M – Cl – Cl – *i*Pr – *i*Pr]$^+$, 275 (100) [M – Cl – Cl – *i*Pr – *i*Pr – C_2H_3O]$^+$. HRMS (EI): calcd. for $C_{18}H_{26}{}^{35}Cl^{37}ClN_2O_3Cr$ [M – Cl]$^+$ 442.0696; found 442.0699. HRMS (EI): calcd. for $C_{18}H_{26}{}^{35}Cl_2N_2O_3Cr$ 440.0426; found 440.0704. $C_{18}H_{26}Cl_3N_2CrO_3$ (476.77): calcd. C 45.3, H 5.5, N 5.9; found C 45.5, H 5.4, N 5.9.

Computational Studies: All the molecular structures were optimized by using the nonlocal hybrid density functional B3PW91[15] with a 6-31g(d) basis set for the C, N, O, Cl and H atoms[16] and the Stuttgart-Dresden effective small core potential basis set for the Ni(SDD) atoms[17] by using the GAUSSIAN03 program package.[18] Electronic structures were studied by using molecular orbitals (MO) and all the orbital visualizations were obtained with GaussView, Chemcraft and Molekel programs.[19] The molecular systems were optimized form X-ray diffraction data as input. Stationary points were verified by frequency. Additionally, the molecular structures of the ligands were fully optimized by using a polarizable continuum model (PCM) with the use of chlorobenzene as the solvent.[20]

X-ray Crystal Structure Determinations: Crystal data and details of the structure determinations are listed in Table 2. Intensity data were collected at 100 K with a Bruker AXS Smart 1000 CCD diffractometer (Mo-K_α radiation, graphite monochromator, λ = 0.71073 Å). Data were corrected for air and detector absorption, Lorentz and polarization effects;[21] absorption by the crystal was treated with a semiempirical multiscan method.[22,23] The structures were solved by conventional direct methods[24] or by the heavy atom method combined with structure expansion by direct methods applied to difference structure factors[25] and refined by full-matrix least-squares methods based on F^2 against all unique reflections.[26] All non-hydrogen atoms were given anisotropic displacement parameters. Hydrogen atoms were generally placed at calculated positions and refined with a riding model. In the structure of complex **5** all hydrogen atoms except those of the methyl groups were taken from difference Fourier syntheses and refined. Complex **6** crystallized as a dichloromethane solvate **6**·CH_2Cl_2 with two independent formula units in the asymmetric unit. Disordered solvent of crystallization was subjected to appropriate geometry restraints. CCDC-736416 (for **5**), -736417 (for **6**), -736418 (for **7**)

Table 2. Details of the crystal structure determinations of complexes **5**, **6**, **7** and **8**.

	5	**6**	**7**	**8**
Formula	$C_{18}H_{26}ClN_3NiO_2$	$C_{20}H_{29}N_3NiO_4{\cdot}CH_2Cl_2$	$C_{18}H_{26}ClN_3NiO_2$	$C_{18}H_{26}Cl_3CrN_2O_3$
Crystal system	monoclinic	monoclinic	orthorhombic	tetragonal
Space group	$P2_1$	$P2_1$	$P2_12_12_1$	$P4_12_12$
a [Å]	8.9948(5)	12.0330(11)	8.2141(5)	7.6937(12)
b [Å]	7.5855(4)	10.3053(9)	12.9149(7)	
c [Å]	13.8206(8)	19.0299(18)	17.5075(10)	36.774(8)
b [°]	90.151(1)	94.767(2)		
V [Å^3]	942.98(9)	2351.6(4)	1857.3(2)	2176.7(7)
Z	2	4	4	4
M_r	410.58	519.10	410.58	476.76
F(000)	432	1088	864	988
$D_{calcd.}$ [Mg m^{-3}]	1.446	1.466	1.468	1.455
m(Mo-K_α) [mm^{-1}]	1.187	1.084	1.205	0.914
Max., min. transmission factors	0.7464, 0.6551	0.7464, 0.6603	0.7464, 0.6518	0.7464, 0.4925
q range [°]	2.3 to 32.2	1.9 to 26.7	2.0 to 30.5	2.2 to 25.0
Index ranges (indep. set) *h*, *k*, *l*	–13 to 13, –11 to 11, 0 to 20	–15 to 15, –13 to 12, 0 to 24	–11 to 11, 0 to 18, 0 to 25	–5 to 6, 0 to 9, 0 to 43
Reflections measured	19084	43154	42002	69323
Unique [R_{int}]	6083 [0.0348]	9946 [0.0625]	5666 [0.0561]	1921 [0.1313]
Observed [$I \geq 2s(I)$]	5347	8129	4811	1829
Parameters refined	276	579	230	127
GooF on F^2	1.05	1.07	1.05	1.19
R indices [$F>4s(F)$] $R(F)$, $wR(F^2)$	0.0339, 0.0705	0.0586, 0.1504	0.0398, 0.0993	0.0613, 0.1418
R indices (all data) $R(F)$, $wR(F^2)$	0.0445, 0.0746	0.0750, 0.1597	0.0500, 0.1055	0.0628, 0.1431
Absolute structure parameter	–0.006(9)	0.008(17)	–0.029(14)	0.01(5)
Largest residual peaks [e Å^{-3}]	0.56, –0.31	1.31, –1.75	1.25, –0.52	1.21, –0.74

and -736419 (for **8**) contain the supplementary crystallographic data for this paper. These data can be obtained free of charge from The Cambridge Crystallographic Data Centre via www.ccdc.cam.ac.uk/data_request/cif.

Supporting Information (see footnote on the first page of this article): NMR study of the proton deuterium exchange in **4a** by AcOD; computational studies; theoretically modelled reaction pathway for the ligand rearrangement mediated by acetic acid (from **4a** to *iso*-**4a**); computed AcOH-mediated rearrangement pathway for the transformation of $\mathbf{5}_{(OAc)}$(AcOH) into **6**(AcOH); Cartesian coordinates of the optimized structures; additional computed rearrangement pathways.

Acknowledgments

We thank the Deutsche Forschungsgemeinschaft (SFB 623) for financial support of this work.

[1] a) Y. Motoyama, N. Makihara, Y. Mikami, K. Aoki, H. Nishiyama, *Chem. Lett.* **1997**, 951; for a review, see: b) H. Nishiyama, *Chem. Soc. Rev.* **2007**, *36*, 1133.

[2] Reviews covering "pincer" complex chemistry: a) M. Albrecht, G. van Koten, *Angew. Chem. Int. Ed.* **2001**, *40*, 3750; b) M. van der Boom, D. Milstein, *Chem. Rev.* **2003**, *103*, 1759; selected references for chiral pincer-based catalysts: c) B. S. Williams, P. Dani, M. Lutz, A. L. Spek, G. van Koten, *Helv. Chim. Acta* **2001**, *84*, 3519; d) B. Soro, S. Stoccoro, G. Minghetti, A. Zucca, M. A. Cinellu, M. Manassero, S. Gladiali, *Inorg. Chim. Acta* **2006**, *359*, 1879; e) J. Aydin, K. S. Kumar, M. J. Sayah, O. A. Wallner, K. J. Szabo, *J. Org. Chem.* **2007**, *72*, 4689; f) B. K. Langlotz, H. Wadepohl, L. H. Gade, *Angew. Chem. Int. Ed.* **2008**, *47*, 4670.

[3] a) H. Nishiyama, H. Sakaguchi, T. Nakamura, M. Horihata, M. Kondo, K. Itoh, *Organometallics* **1989**, *8*, 846; b) H. Nishiyama, M. Kondo, T. Nakamura, K. Itoh, *Organometallics* **1991**, *10*, 500; c) H. Nishiyama, *Advances in Catalytic Processes* (Ed.: M. P. Doyle), JAI, Greenwich, CT, **1997**, vol. 2, p. 153.

[4] a) T. Suzuki, A. Kinoshita, H. Kawada, M. Nakada, *Synlett* **2003**, 570; b) M. Inoue, M. Nakada, *Heterocycles* **2007**, *72*, 133; c) M. Inoue, T. Suzuki, A. Kinoshita, M. Nakada, *Chem. Rec.* **2008**, *8*, 169; d) M. Inoue, T. Suzuki, M. Nakada, *J. Am. Chem. Soc.* **2003**, *125*, 1140.

[5] S. Kanemasa, Y. Oderatoshi, H. Yamamoto, J. Tanaky, E. Wada, D. Curran, *J. Org. Chem.* **1997**, *62*, 6454.

[6] A. Voituriez, J.-C. Fiaud, E. Schulz, *Tetrahedron Lett.* **2002**, *43*, 4907.

[7] C. Mazet, L. H. Gade, *Chem. Eur. J.* **2003**, *9*, 1759.

[8] F. Konrad, J. Lloret Fillol, H. Wadepohl, L. H. Gade, *Inorg. Chem.* **2009**, *48*, 8523.

[9] a) R. Li, D. S. Larsen, S. Brooker, *New J. Chem.* **2003**, *27*, 1353. This synthetic route is in part based on previous work by: b) F. Johnson, K. G. Paul, D. Favara, R. Ciabatti, U. Guzzi, *J. Am. Chem. Soc.* **1982**, *104*, 2190; c) W. Flitsch, F.-J. Lüttig, *Liebigs Ann. Chem.* **1987**, 893. See also: d) J.-M. Simone, F. Loiseau, D. Carcache, P. Bobal, J. Jeanneret-Gris, R. Neier, *Monatsh. Chem.* **2007**, *138*, 141; e) W. Flitsch, J. Schweizer, U. Strunk, *Justus Liebigs Ann. Chem.* **1975**, 1967.

[10] a) J. Bourguignon, U. Bremberg, G. Dupas, K. Hallman, L. Hagberg, L. Hortala, V. Levacher, S. Lutseko, E. Macedo, C. Moberg, G. Quéguiner, F. Rahm, *Tetrahedron* **2003**, *59*, 9583; b) S. Dagorne, S. Bellemin-Laponnaz, R. Welter, *Organometallics* **2004**, *23*, 3053; c) C. Foltz, M. Enders, S. Bellemin-Laponnaz, H. Wadepohl, L. H. Gade, *Chem. Eur. J.* **2007**, *13*, 5994.

[11] T. Oshima, T. Iwasaki, K. Mashima, *Chem. Commun.* **2006**, 2711.

[12] R. B. Woodward, R. Hoffmann, *Angew. Chem. Int. Ed. Engl.* **1969**, *8*, 781.

[13] B. Bak, D. Christansen, L. Hansen, J. Rastrup-Andersen, *J. Chem. Phys.* **1956**, *24*, 720.

[14] a) F. H. Allen, O. Kennard, *Chem. Des. Automation News* **1993**, *8*, 1; F. H. Allen, O. Kennard, *Chem. Des. Automation News* **1993**, *8*, 31;b) D. A. Fletcher, R. F. McMeeking, D. J. Parkin, *J. Chem. Inf. Comput. Sci.* **1996**, *36*, 746.

[15] a) A. D. Becke, *J. Chem. Phys.* **1993**, *98*, 5648; b) J. P. Perdew, Y. Wang, *Phys. Rev. B* **1992**, *45*, 13244.

[16] a) W. J. Hehre, R. Ditchfield, J. A. Pople, *J. Chem. Phys.* **1972**, *56*, 2257; b) P. C. Hariharan, J. A. Pople, *Theor. Chim. Acta* **1973**, *28*, 213; c) J. A. Pople, *J. Chem. Phys.* **1975**, *62*, 2921; d) M. M. Francl, W. J. Petro, W. J. Hehre, J. S. Binkley, M. S. Gordon, D. J. DeFrees, J. A. Pople, *J. Chem. Phys.* **1982**, *77*, 3654; e) T. Clark, J. Chandrasekhar, G. W. Spitznagel, P. v. R. Schleyer, *J. Comput. Chem.* **1983**, *4*, 294.

[17] M. Dolg, H. Stoll, H. Preuss, R. M. Pitzer, *J. Chem. Phys.* **1993**, *97*, 5852.

[18] M. J. Frisch, G. W. Trucks, H. B. Schlegel, G. E. Scuseria, M. A. Robb, J. R. Cheeseman, J. A. Montgomery Jr., T. Vreven, K. N. Kudin, J. C. Burant, J. M. Millam, S. S. Iyengar, J. Tomasi, V. Barone, B. Mennucci, M. Cossi, G. Scalmani, N. Rega, G. A. Petersson, H. Nakatsuji, M. Hada, M. Ehara, K. Toyota, R. Fukuda, J. Hasegawa, M. Ishida, T. Nakajima, Y. Honda, O. Kitao, H. Nakai, M. Klene, X. Li, J. E. Knox, H. P. Hratchian, J. B. Cross, V. Bakken, C. Adamo, J. Jaramillo, R. Gomperts, R. E. Stratmann, O. Yazyev, A. J. Austin, R. Cammi, C. Pomelli, J. W. Ochterski, P. Y. Ayala, K. Morokuma, G. A. Voth, P. Salvador, J. J. Dannenberg, V. G. Zakrzewski, S. Dapprich, A. D. Daniels, M. C. Strain, O. Farkas, D. K. Malick, A. D. Rabuck, K. Raghavachari, J. B. Foresman, J. V. Ortiz, Q. Cui, A. G. Baboul, S. Clifford, J. Cioslowski, B. B. Stefanov, G. Liu, A. Liashenko, P. Piskorz, I. Komaromi, R. L. Martin, D. J. Fox, T. Keith, M. A. Al-Laham, C. Y. Peng, A. Nanayakkara, M. Challacombe, P. M. W. Gill, B. Johnson, W. Chen, M. W. Wong, C. Gonzalez, J. A. Pople *Gaussian 03*, revision D.02, Gaussian, Inc., Wallingford, CT, **2004**.

[19] a) R. Dennington, T. Keith, J. Millam, K. Eppinnett, W. L. Hovell, R. Gilliland, *GaussView*, version 3.0, Semichem, Inc., Shawnee Mission, KS, **2003**; b) http://www.chemcraftprog.com; c) P. Flükiger, H. P. Lüthi, H. Portmann, S. J. Weber, *MOLEKEL 4.0*, Swiss National Supercomputing Centre CSCS, Mann o, Switzerland, **2000**.

[20] M. Cossi, V. Barone, R. Cammi, J. Tomasi, *Chem. Phys. Lett.* **1996**, *255*, 327.

[21] *SAINT*, Bruker AXS, **2007**.

[22] R. H. Blessing, *Acta Crystallogr., Sect. A* **1995**, *51*, 33.

[23] G. M. Sheldrick, *SADABS*, Bruker AXS, **2004–2008**.

[24] a) G. M. Sheldrick, *SHELXS-86*, University of Göttingen, Germany, **1986**; b) G. M. Sheldrick, *Acta Crystallogr., Sect. A* **1990**, *46*, 467.

[25] P. T. Beurskens, *Crystallographic Computing 3* (Eds.: G. M. Sheldrick, C. Krüger, R. Goddard), Clarendon Press, Oxford, UK, **1985**, p. 216; P. T. Beurskens, G. Beurskens, R. de Gelder, J. M. M. Smits, S. Garcia-Granda, R. O. Gould, *DIRDIF-2008*, Radboud University Nijmegen, The Netherlands, **2008**.

[26] a) G. M. Sheldrick, *SHELXL-97*, University of Göttingen, **1997**; b) G. M. Sheldrick, *Acta Crystallogr., Sect. A* **2008**, *64*, 112.

Received: August 13, 2009
Published Online: October 22, 2009

